PARTICLE ACCELERATION BY THE SUN: ELECTRONS, HARD X-RAYS/GAMMA-RAYS

R. P. LIN
Physics Department & Space Sciences Laboratory, University of California, Berkeley, CA 94720-7450, USA
(E-mail: rlin@ssl.berkeley.edu)

(Received 15 June 2006; Accepted in final form 26 July 2006)

Abstract. Observations of hard X-ray (HXR)/γ-ray continuum and γ-ray lines produced by energetic electrons and ions, respectively, colliding with the solar atmosphere, have shown that large solar flares can accelerate ions up to many GeV and electrons up to hundreds of MeV. Solar energetic particles (SEPs) are observed by spacecraft near 1 AU and by ground-based instrumentation to extend up to similar energies, but it appears that a different acceleration process, one associated with fast Coronal Mass Ejections (CMEs) is responsible. Much weaker SEP events are observed that are generally rich in electrons, ^{3}He, and heavy elements. The energetic particles in these events appear to be similar to those accelerated in flares. The Ramaty High Energy Solar Spectroscopic Imager (RHESSI) mission provides high-resolution spectroscopy and imaging of flare HXRs and γ-rays. The observations of the location, energy spectra, and composition of the flare accelerated energetic particles at the Sun strongly imply that the acceleration is closely related to the magnetic reconnection that releases the energy in solar flares. Here preliminary comparisons of the RHESSI observations with observations of both energetic electrons and ions near 1 AU are reviewed, and the implications for the particle acceleration and escape processes are discussed.

Keywords: electrons, solar energetic particles, flares, SEPs, radio, hard X-rays, RHESSI, WIND

1. Introduction

In large solar flares, nuclear γ-ray lines and pion decay emission have been detected that are produced by energetic ions with ~10–100 MeV and GeV energies, respectively, in nuclear collisions with the solar atmosphere (Lin *et al.*, 2003). HXR/γ-ray continuum emissions, produced by bremsstrahlung collisions of energetic electrons with the atmosphere, have been observed up to $\gtrsim$100 MeV. Ions and electrons up to about the same energies have been directly detected by *in situ* space observations (ground-based observations for the most energetic ions) in the interplanetary medium (IPM) near 1 AU in solar energetic particle (SEP) events. Somewhat surprisingly, the energetic ions and electrons that produce the HXR and γ-ray emissions in solar flares appear to be accelerated by a different process than the SEPs observed near 1 AU – those appear associated with fast coronal mass ejections (CMEs) and the shocks they drive, or possibly by high coronal acceleration processes. These extremely energetic particle acceleration phenomena are associated with enormous transient releases of energy, $\gtrsim 10^{32}$ ergs for large solar

Space Science Reviews (2006) 124: 233–248
DOI: 10.1007/s11214-006-9107-9

flares, with accelerated particles containing a significant fraction of the total energy released (Lin and Hudson, 1976).

The Sun exhibits a wide range of acceleration phenomena. Flares of all sizes, ranging down to microflares ($\sim 10^{-6}$ the energy release of the largest flares) that occur every few minutes near solar maximum, appear to accelerate electrons (Lin *et al.*, 2001). For flares, the frequency of occurrence increases rapidly as the size decreases, suggesting the possibility that the total averaged energy release might be significant for the heating of the corona.

Solar type III radio bursts are generated by electrons accelerated in the corona that escape to the IPM. A large fraction, perhaps most, of type III bursts are unaccompanied by flares. In the IPM near 1 AU, impulsive electron events are often detected at $\sim$1–100 keV energies, sometimes down to energies of $\sim$0.1 keV. Such low energy electrons must originate high in the corona since energy losses due to Coulomb collisions limit the amount of coronal material they can traverse (Lin *et al.*, 1996). These impulsive events are closely associated with type III bursts that extend into the IPM. The more energetic ($\gtrsim$30 keV) electrons in these events, however, often show delayed onsets that suggest injections $\sim$10 minutes after the type III burst at the Sun.

The relationship between the energetic particles at the Sun and the energetic particles observed near 1 AU is not understood. Here we compare the energetic particle measurements from the Wind, ACE, and other spacecraft near 1 AU with RHESSI observations that provide detailed information on the energetic particle populations in solar flares. In particular, the 28 October and 2 November 2003 large flares were the first for which RHESSI had γ-ray line observations and SEP ions were observed by Wind and near 1 AU. In addition, we summarize the comparisons between RHESSI hard X-rays observations and energetic electron observations from Wind.

2. RHESSI Hard X-Ray/γ-Ray Observations of Solar Flares

The NASA Reuven Ramaty High Energy Solar Spectroscopic Imager (RHESSI) mission (Lin *et al.*, 2002), launched on February 5, 2002, provides high resolution imaging and spectroscopy from soft X-rays (3 keV) to γ-rays (17 MeV). The RHESSI imager (Hurford *et al.*, 2002) is made up of nine bi-grid rotating modulation collimators (RMCs), each consisting of a pair of widely separated grids mounted on a rotating spacecraft, to provide spatial resolution of 2.3 arcsec to 3 arcmin over the full Sun ($\sim 1^{\circ}$) field of view. Behind each RMC is a coaxial germanium detector (GeD), cooled to $\sim$80 K to achieve spectral resolution of $\sim$1 keV FWHM for HXRs, increasing to $\sim$4 keV FWHM at $\sim$2 MeV, the best ever achieved for solar measurements.

The first γ-ray line flare observed by RHESSI was the intense GOES class X4.8 flare of 23 July 2002 (Lin *et al.*, 2003). The flare HXR and γ-ray observations

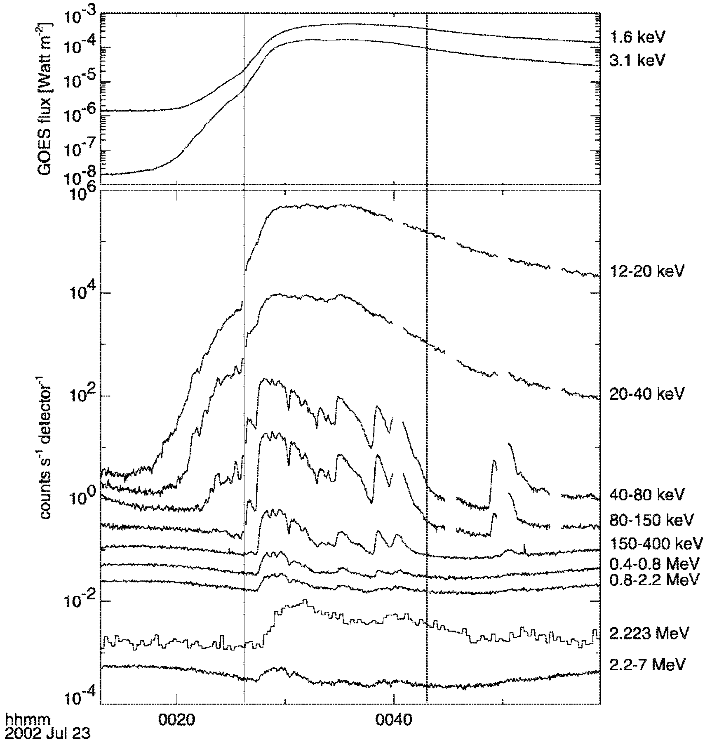

Figure 1. RHESSI HXR and γ-ray count rates (in units of counts s^{-1} per detector) for the 2002 July 23 flare, scaled to fit: 20–40 keV $\times$ 0.3; 40–80 keV $\times$ 0.07; 80–150 keV $\times$ 0.02; 150–400 keV; 400–800 keV $\times$ 0.001; 800–2218 keV $\times$ 0.0005; 2218–2228 keV $\times$ 0.01; and 2228–7000 $\times 2 \times 10^{-5}$. The thick shutter is inserted at ~0026, 0041, 0044, and 0050 UT and removed at ~0040, 0043, 0049 UT. The vertical lines separate the impulsive phase from the rise and decay. The slow variation of the γ-ray rates through the interval is due to the background from cosmic-ray interactions with the atmosphere and spacecraft (Lin *et al.*, 2003).

(Figure 1) divide naturally into a rise phase (~00:18 to ~00:27 UT) dominated by a coronal HXR source that appears to be non-thermal, an impulsive phase (~00:27 to ~00:43 UT) with continuum and γ-ray line emission extending up to $\gtrsim$7 MeV, and a decay phase ($\gtrsim$00:43 UT) dominated by a superhot (~40 MK) thermal source. The spatial distribution of HXR sources (Krucker *et al.*, 2003) is shown superimposed on TRACE 195 Å images, together with the simultaneous spatially integrated X-ray spectra, in a movie at: `http://hesperia.gsfc.nasa.gov/hessi/presentations/video/`.

A remarkable coronal hard X-ray source with a steep double power-law spectrum above 10 keV (exponents γ_L ~5 and γ_H ~6.5, with break at 20–35 keV) dominates the flare X-ray emission during the rise before the impulsive phase. Little or no footpoint emission (or TRACE emission in the lower corona) is detected through most of this period. The energy in accelerated electrons during

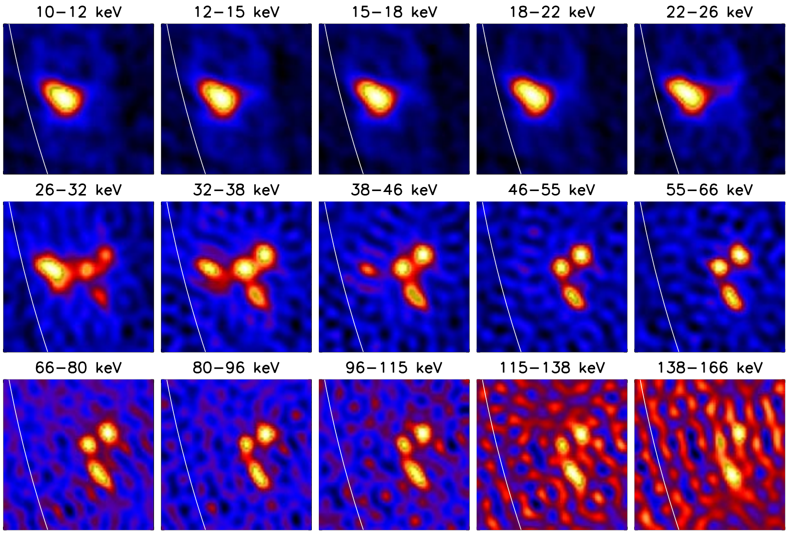

Figure 2. RHESSI X-ray images in different energy bands for a 20 s interval during the impulsive phase of the 23 July 2002 flare. At energies up to 26 keV, only the hot coronal thermal source is visible. Above that energy, the three (possibly more) non-thermal footpoint sources are observed (Emslie *et al.*, 2003).

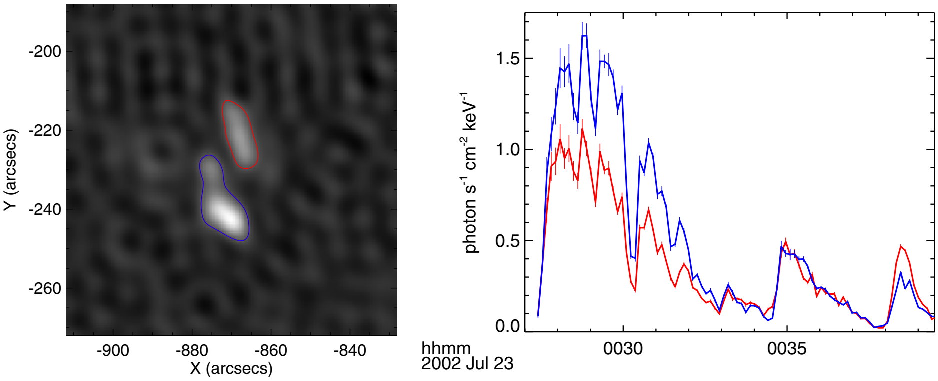

Figure 3. Left panel: RHESSI image at 100–200 keV, showing two main footpoints for the 23 July 2002 flare. The circles define the regions for which the count rates shown in the bottom panel are accumulated. Right panel: the count rates for the two regions are plotted as a function of time. The close correlation in time of the count rates for the two regions strongly suggest that they are opposite ends of a loop that is being fed by a single source of energetic electrons (Krucker *et al.*, 2003).

this time, however, is significant, comparable to that released in the impulsive phase.

During this flare's impulsive phase, RHESSI's detailed hard X-ray imaging spectroscopy show three footpoint sources (Figure 2), together with a coronal superhot ($T \sim 40$ MK) thermal source that dominates below ~30 keV. The temporal

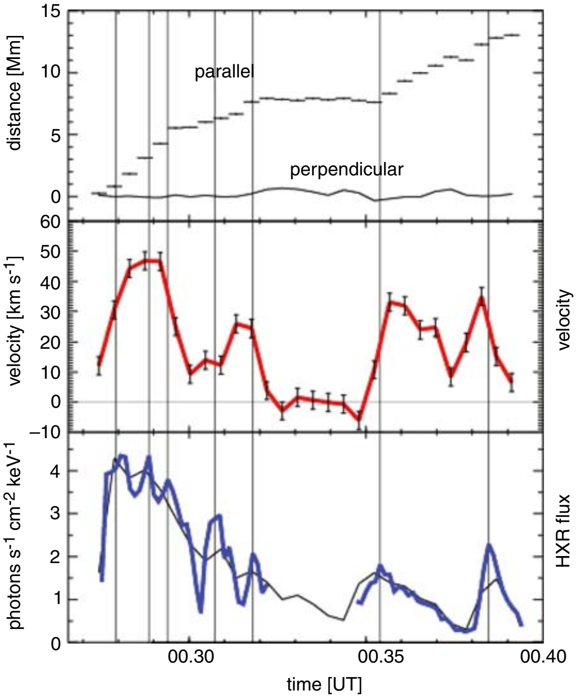

Figure 4. The motion of the two main footpoints for the 23 July 2002 flare observed by RHESSI. Top panel the position of the moving footpoint versus time. Center panel: The speed computed from the top panel versus time. Bottom panel: the hard X-ray flux versus time. A rough correlation is evident between the speed and hard X-ray flux (Krucker *et al.*, 2003).

variations of the hard X-ray fluxes of the different foot points are closely correlated (Figure 3), and the footpoints and coronal source show correlated and systematic motions, strongly suggesting magnetic reconnection in the corona, possibly at or near the thermal coronal source. Furthermore, the footpoint X-ray fluxes are found to be approximately proportional to the footpoint separation speed (Figure 4), as expected if the rate of electron acceleration is proportional to the reconnection rate.

Gamma-ray line and continuum emission show that ions are accelerated to tens of MeV and electrons to $\gtrsim$7 MeV. The prompt de-excitation γ-ray lines of Fe, Mg, Si, Ne, C, and O show mass-dependent red shifts of 0.1–0.8%, implying downward motion of accelerated protons and alphas along magnetic field lines that are not radial, but tilted toward the Earth by $\sim$40° (Smith *et al.*, 2003). RHESSI made the first γ-ray line imaging for a flare (Hurford *et al.*, 2003), showing that the accelerated ions interact in a region near the optical flare (Figure 5). The centroid of the 2.223 MeV neutron capture line emission, however, is located $\sim 20 \pm 6$ arcseconds from the centroids for the 0.3–0.5 and 0.7–1.4 MeV bands that are dominated by electron bremsstrahlung, implying that the acceleration and/or propagation of the accelerated ions must differ from that of the electrons.

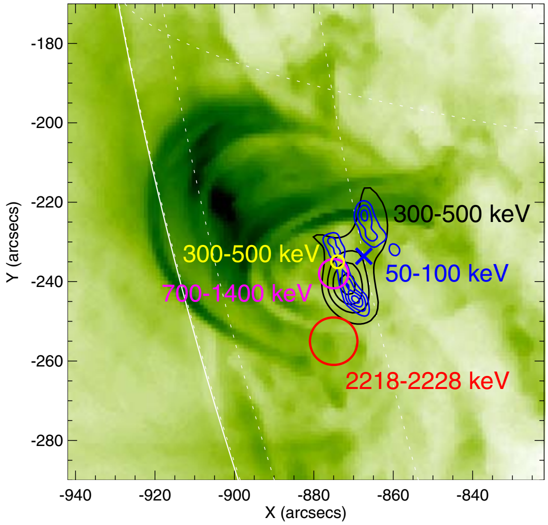

Figure 5. The first image of a flare in a γ-ray line, obtained by RHESSI for the 23 July 2002 flare in the 2.223 MeV neutron-capture line (Hurford *et al.*, 2003). The red circle shows the centroid of the flare-averaged 2.223 MeV line image, superimposed on a TRACE image taken well after the flare. The blue contours show the flare-averaged hard X-ray image at 50–100 keV. The black contour shows the flare-averaged continuum image at 300–500 keV. The yellow and red circles show the centroid of the 300–500 keV and 700–1400 keV continuum, respectively, obtained through the same grids as the 2.223 MeV image.

Assuming that Coulomb collisions dominate the energetic electron and ion energy losses (thick-target) we estimate a minimum of $\sim 2 \times 10^{31}$ ergs is released in accelerated >18 keV electrons during the rise phase, with $\sim 10^{31}$ ergs in ions above 2.5 MeV and about the same in electrons above 30 keV released in the impulsive phase. There could be much more energy in accelerated particles if their spectra extends to lower energies.

Recently, RHESSI imaging of three more flares (28, 29 October and 2 November 2003) in the 2.223 MeV neutron-capture γ-ray line was reported (Hurford *et al.*, 2006). Comparison of imaged and spatially-integrated fluences show that in all these flares (including 23 July 2002) most, if not all, of the emission was confined to compact sources with size scales of tens of arcsec or smaller, that are located in the flare active region. Thus, the γ-ray producing ions appear to be accelerated by the flare process and not by a widespread shock driven by a fast coronal mass ejection. The 28 October 2003 event yielded the first of such images to show double-footpoint γ-ray line sources (Figure 6), similar to what is seen in the hard X-ray image, and strongly supporting a similar flare origin for the ion acceleration. These foot-point sources straddled the flaring loop arcade but were displaced from the corresponding 0.2–0.3 MeV electron-bremsstrahlung emission footpoints by 14 and 17 $\pm$ 5 arcsec. Taken together with the previously studied 23 July 2002

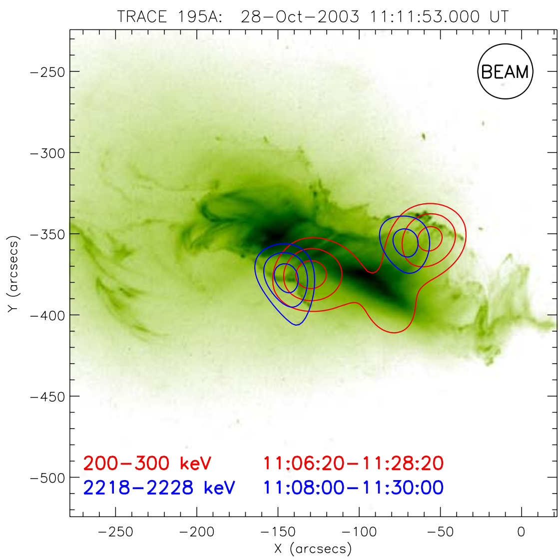

Figure 6. RHESSI γ-ray line image of the 28 October 2003 solar flare (Hurford *et al.*, 2006). The blue contours show the flare-averaged (RHESSI was in shadow for the first few minutes of the flare) 2.223 MeV neutron-capture γ-ray line (produced by 10–100 MeV ions) image, together with the 200–300 keV hard X-ray continuum (produced by energetic electrons) image made through the same grids and using the same analysis procedure. The angular resolution is indicated by beam circle (upper right). The accelerated electrons and ions appear to be separated by ~10,000 km.

event where the centroid of the γ-ray line source is displaced by $\sim 25 \pm 5$ arcsec from the centroid of the electron bremsstrahlung source, this implies spatial differences in acceleration and/or propagation between ions and electrons in solar flares.

In many flares the coronal thermal sources observed by RHESSI above the lower temperature loops seen by TRACE move upward with time, suggesting the energy release site moves to high altitudes with time, in agreement with classical flare models (Sturrock, 1966; Shibata *et al.*, 1995). In the 21 April 2002 flare the onset of the flare and thermal source motions is well correlated with the beginning of the associated CME (Gallagher *et al.*, 2002).

In some flares a second much weaker coronal source is detected above the normal thermal source (Sui and Holman, 2003). The centroids of the two sources, obtained at energies from ~8 to >20 keV, show a systematic behavior with the most energetic centroids located closest to the region in between the two sources (Figure 7), with less and less energetic centroids the further away from that point. This is consistent with a temperature gradient away from that point, suggesting a large scale current sheet with energy release from magnetic reconnection in the region in between, again consistent with the Shibata *et al.* (1995) classical flare model.

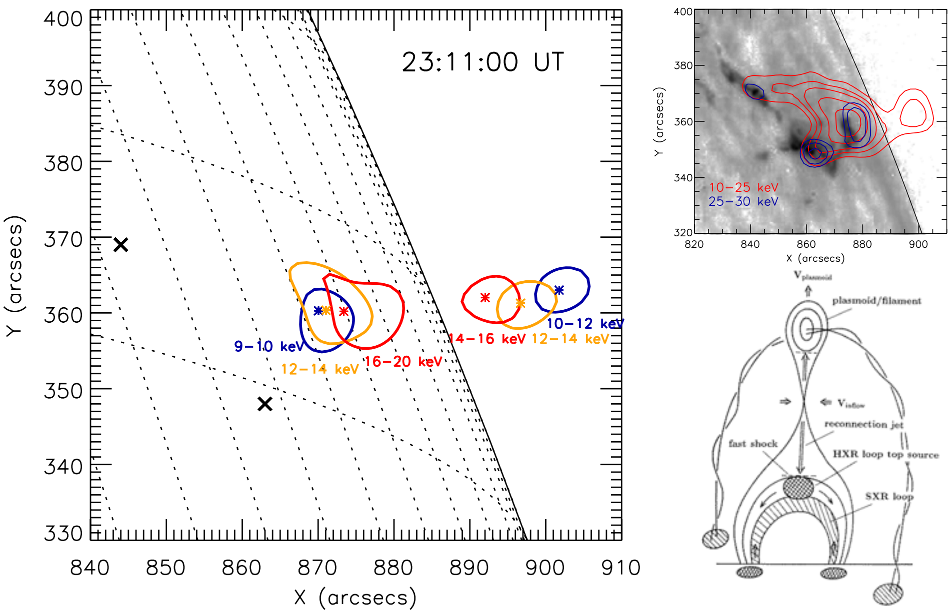

Figure 7. RHESSI imaging of the hot flare plasma above the flare loop, showing evidence for a large scale current sheet. The centroids of the sources at different energies indicate a temperature gradient both upward and downward from the center (Sui and Holman, 2003), as expected in models of flares where magnetic reconnection occurs in the current sheet. The $\times$'s indicate where the hard X-ray footpoints are located.

3. Energetic Ions at the Sun and SEPs at 1 AU

RHESSI has detected γ-ray line emission from about a dozen solar flares to date, with SEP events detected near 1 AU for three of them. A major SEP event occurred following the 21 April 2002 flare that was well observed by RHESSI (Gallagher *et al.*, 2002), but no γ-ray line emission was detected, indicating that no significant acceleration of energetic ($\gtrsim$10 MeV) ions occurred in the flare. The flare and CME initiation were closely related in time, with the impulsive hard X-ray emission starting the whole process.

The flare on 23 July 2002 was accompanied by a very fast (2180 km/s) and wide CME. Since it was located at S13 E72 near the east limb of the Sun, it was not surprising that no SEPs were detected by the ACE or Wind spacecraft near the Earth. No SEPs were detected by the Mars Global Surveyor (MGS) spacecraft located on the opposite side of the solar system very close to the nominal Parker spiral field from the flare region, however, even though two previous SEP events (July 16 and 19) were detected from the same active region. This suggests that even a very fast and wide CME may not always accelerate SEPs.

SEP events were detected from the 28 October 2003, 29 October 2003, and 2 November 2003 γ-ray line flares observed by RHESSI. For 28 October 2003 and 2

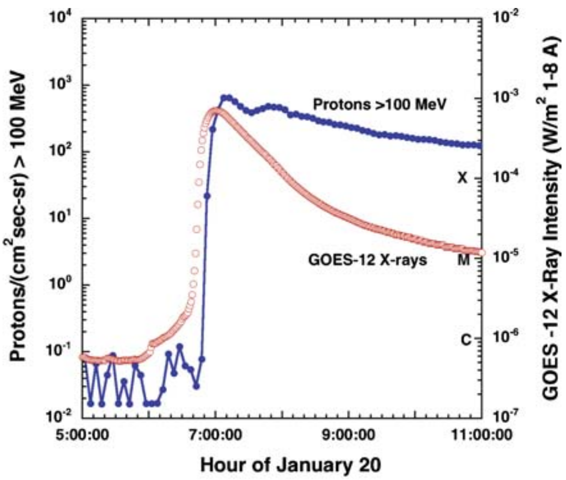

Figure 8. In the solar energetic particle event of 20 January 2005 the 100 MeV protons arrive and reach peak intensity within minutes of the GOES soft X-ray peak for the flare.

November 2003, the spectra of energetic protons were obtained from the observed narrow line fluences of the 2.223 MeV neutron-capture line and the 4.443 MeV carbon line (Ramaty and Murphy, 1987). (During the 29 October 2003 flare, RHESSI passed close to the South Atlantic Anomaly so the background is high and the line fluences uncertain.) These can be compared to the number and power law exponent for the energetic protons observed near 1 AU (using ACE, GOES 10, and SAMPEX spacecraft to provide full energy coverage), integrating over the entire event to obtain the fluences. The observed proton spectra are double power-law with a downward break at ∼20–30 MeV. The integrated fluence will probably overestimate the number of particles accelerated/injected near the Sun, since scattering in the interplanetary medium will allow some particles to cross 1 AU distance more than once (Li *et al.*, 2003).

The spectral exponents for the γ-ray producing protons and the protons at 1 AU are essentially the same for the magnetically well-connected 2 November 2003 event, within measurement uncertainties, but different for the 28 October 2003. Furthermore, very preliminary estimates of the Ne line fluences, which are sensitive to protons down to ∼2.5 MeV, indicate that they are unusually low, suggesting that the γ-ray producing proton spectrum flattens at low energies, similar to what is observed for the protons detected at 1 AU.

More recently RHESSI observed γ-ray line emission from the flare associated with the 20 January 2005 event, the most intense SEP event detected in nearly five decades, at energies above a few hundred MeV. The SEPs arrive within minutes after the flare X-ray peak (Figure 8), raising questions about the role of CME shock acceleration. The very limited CME observations (the SOHO coronagraph was quickly saturated by the penetrating SEPs!) indicate that the CME velocity in this event ranged from ~2500 to ~3500 km/s (Mewaldt *et al*., 2005; Gopalswamy *et al*., 2005), implying that the CME was only $\lesssim 2R_s$ above the solar surface when the first GeV protons were released. It is uncertain whether a shock could form and accelerate particles to GeV energies in the short time and distance available (Kahler, 2005). Finally, it is interesting that in the 20 January 2005 event (also magnetically well-connected) both the flare-accelerated proton spectrum from ~10 to ~100 MeV (as derived from RHESSI γ-ray observations) and the proton spectrum at 1 AU (derived from SAMPEX, ACE, and GOES data) are similar, both as hard as or harder than any spectra observed using these techniques (Share, personal communication). The implications of these observations for the relative roles of flare acceleration and shock acceleration in this event are not clear. Given that our current understanding is that the γ-ray producing protons are accelerated by a different process (flares) from the SEP protons (fast CMEs), this is very surprising.

4. Energetic Electrons at the Sun and at 1 AU

Electrons accelerated at the Sun and interacting with the solar atmosphere will produce hard X-rays through bremsstrahlung collisions, and radio emission through wave-particle interactions and through synchrotron emission. As the faster electrons run ahead of the slower ones when the impulsively accelerated electrons escape from the Sun, bump-on-tail distributions will be generated that are unstable to the growth of Langmuir waves. These waves then interact with the ambient plasma or with other waves to produce radio emission at the plasma frequency or its harmonic. As the electrons travel to lower and lower density the radio emission goes to lower frequencies, leading to the characteristic fast drift solar type III radio burst.

If the HXR-producing and escaping electrons come from a single acceleration, a hard X-ray burst should be detected with a near simultaneous type III burst starting at high frequencies. When the type III burst drifts down to near the local plasma frequency at 1 AU, the escaping electrons and Langmuir waves can be directly detected *in situ*. Figure 9a shows an example of this, while Figure 9b shows the flare X-ray spectrum (both thermal and HXR) observed by RHESSI, and the electron spectrum measured by the Wind 3D Plasma & Energetic Particle (3-DP) experiment (Lin *et al*., 1995). Both spectra fit a double power-law with a downward break at a few tens of keV.

Figure 10 shows a comparison of power-law exponents above the break for the electron spectra observed by Wind at 1 AU, with exponents for the HXR photon spectra observed by RHESSI, for ~15 events that have the timing consistent with a single acceleration (Krucker *et al*., 2004). The points should fall on the "Thick" target line if the escaping electrons directly sample the accelerated population (without any energy changes), and the accelerated electrons produce the HXRs as they lose all their energy to Coulomb collisions, i.e., if the acceleration occurs high in the corona and some of the electrons escape to the IPM while the rest are trapped

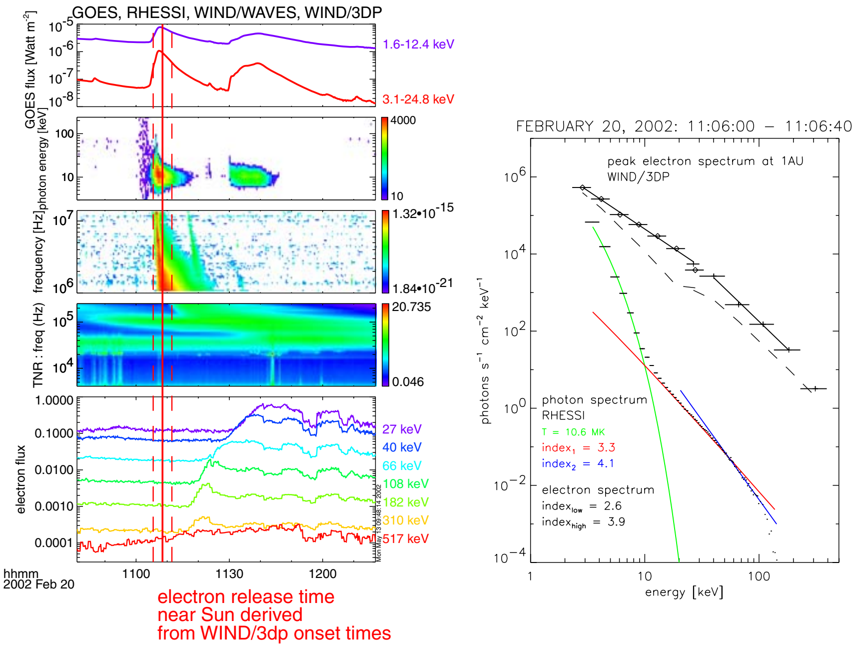

Figure 9. (a) Example of a flare hard X-ray burst observed by RHESSI with corresponding solar type III radio burst and energetic electrons (and Langmuir waves) observed *in situ* by the Wind spacecraft (Krucker and Lin, 2002). Top panel: GOES soft X-rays; second panel: Spectrogram of RHESSI X-rays from 3 to 250 keV; third and fourth panels: radio emission observed by the Wind WAVES instrument; fifth panel: Electrons from ∼20 to ∼400 keV observed by Wind 3-DP instrument. (b) Top trace: energy spectrum of the electrons observed by Wind 3-D P instrument; bottom trace: X-ray spectrum observed by RHESSI, fitted to a thermal spectral shape at low energies, and to a double power-law at high energies (Krucker and Lin, 2002).

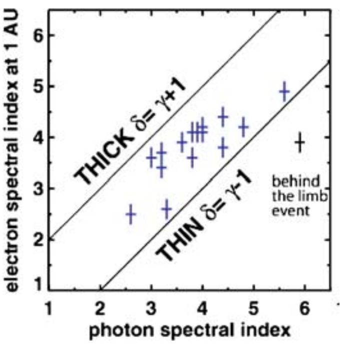

Figure 10. Comparison of power-law exponent for the hard X-ray spectrum at the peak of the burst measured by RHESSI with the power-law exponent for the electron spectrum measured at the time of maximum at each energy. δ and γ are the power-law exponents for the electron and hard X-ray spectra, respectively (Krucker *et al.*, 2004).

in the solar atmosphere. The "Thin" target line would be for the case where the electrons produce the HXRs as they escape, but the collisions are too few to modify the spectrum. The data points appear to show a rough linear correlation with larger electron exponents for larger HXR exponents (with the exception of the behind the limb event), suggesting that the electrons producing the HXRs at the Sun indeed are somehow related to the electrons in these impulsive events observed in the IPM. The RHESSI images typically show the HXRs come from footpoints where the ambient density is high – presumably the electrons are losing their energy to collisions, i.e., thick target. The points, however, do not lie on the "Thick" line or the "Thin" line, indicating that the relationship is more complex than these simple models.

As mentioned above, for many of the impulsive electron events observed at energies of tens of keV, the inferred injection of electrons back at the Sun appears to be delayed by $\sim$10 minutes from the start of the type III radio burst, suggesting acceleration by a coronal or CME shock wave (Krucker *et al.*, 1999; Haggerty and Roelof, 2002). Many impulsive electron events often extend down to below $\sim$1 keV (Lin *et al.*, 1996) and many are detected even in the energy range $\sim$0.1 to $\sim$1 keV (Gosling *et al.*, 2003).

Recently, Wind 3DP observations (which covers from $\sim$1 eV up to $\gtrsim$300 keV electrons) of three scatter-free impulsive electron events with delayed onset at $\gtrsim$30 keV (Haggerty and Roelof, 2002) were carefully analyzed to accurately determine the injection near the Sun (Wang *et al.*, 2006). The event shown in Figure 11 extends down to 0.4 keV, and it shows a rapid, nearly symmetric rise and decay. This indicates essentially scatter-free propagation from the Sun to 1 AU, since scattering would result in a slowly decaying tail in the time profile (Lin, 1974).

A model is applied where the injection time profile is assumed to be triangular, with equal time for rise to the peak and decay back to zero (Figure 12). The injected electrons were assumed to travel $\sim$1.2 AU, the Parker spiral field line length appropriate for the measured $\sim$400 km/s solar wind. Model time profiles were calculated using the measured spectrum of the event and integrating over the width of each energy channel. The injection time and width were then adjusted to fit the observed profile in each energy channel. As can be seen (Figure 12), the injection profiles at energies above $\sim$20 keV are similar, with comparable widths of $\sim$5 minutes. The best-fit injection times are the same at all energies above $\sim$20 keV, confirming that $\sim$1.2 AU is appropriate for the path length. The onset of the injection for $>$20 keV electrons is clearly delayed by $\sim$8 minutes relative to the type III burst injection (dashed vertical line).

A data gap and poor statistics in the $\sim$4 to 20 keV measurements precluded accurate timing for those energies. The inferred injection profiles for $\sim$0.6 to $\sim$3 keV electrons show onsets starting prior to or at the type III burst injection, early enough that they could be the source of the radio emission. Previous *in situ* observations at 1 AU of the Langmuir waves responsible for type III radio emission show that they occur primarily when $\sim$2–12 keV electrons arrive at the spacecraft (Lin, 1985).

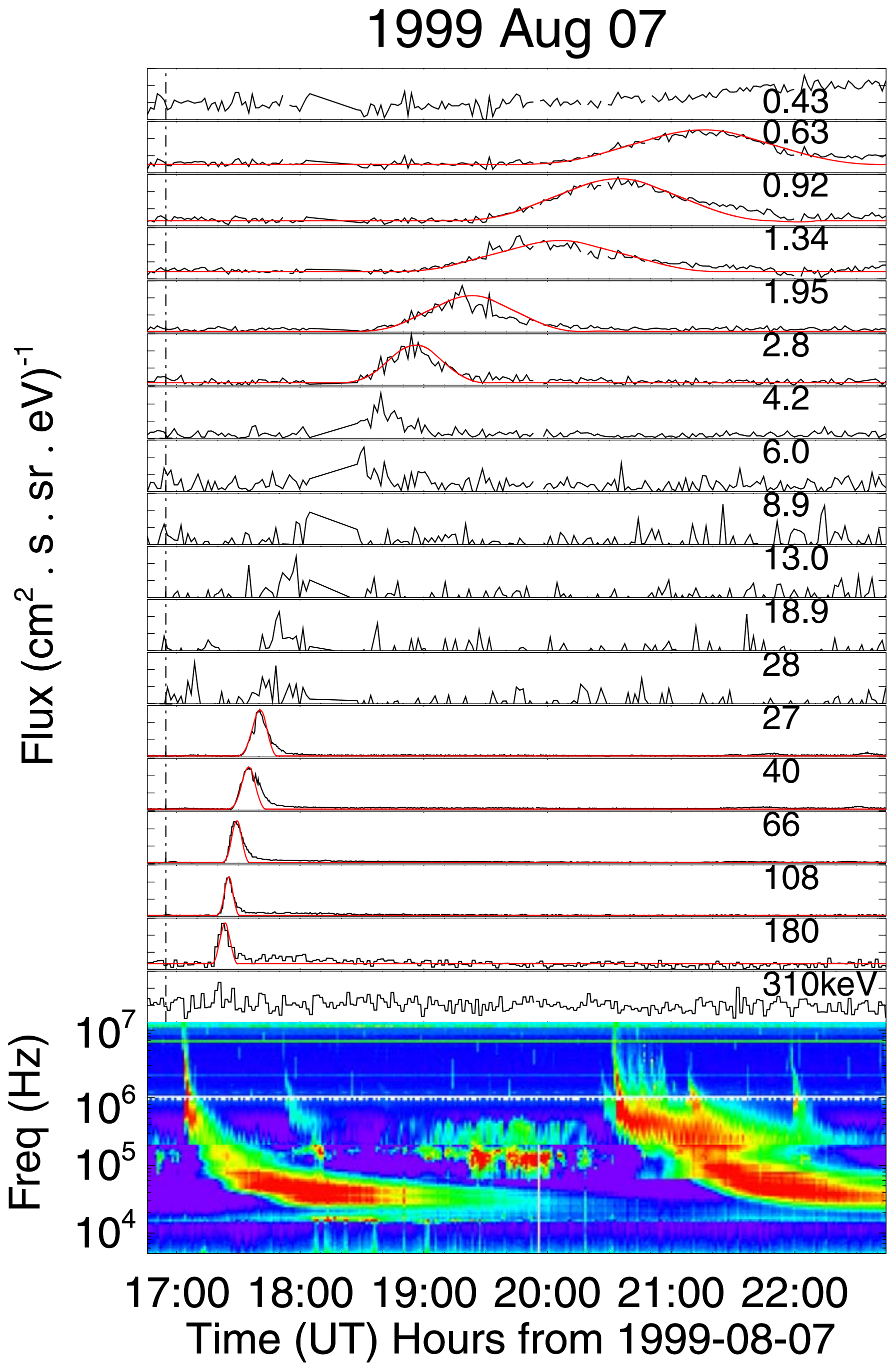

Figure 11. Scatter-free impulsive electron event observed by the Wind 3-D P instrument at energies from 0.1 to 300 keV (top two panels), and radio dynamic spectrum from the Wind WAVES instrument (Wang *et al.*, 2006). The smooth lines show the model fit (see Figure 12).

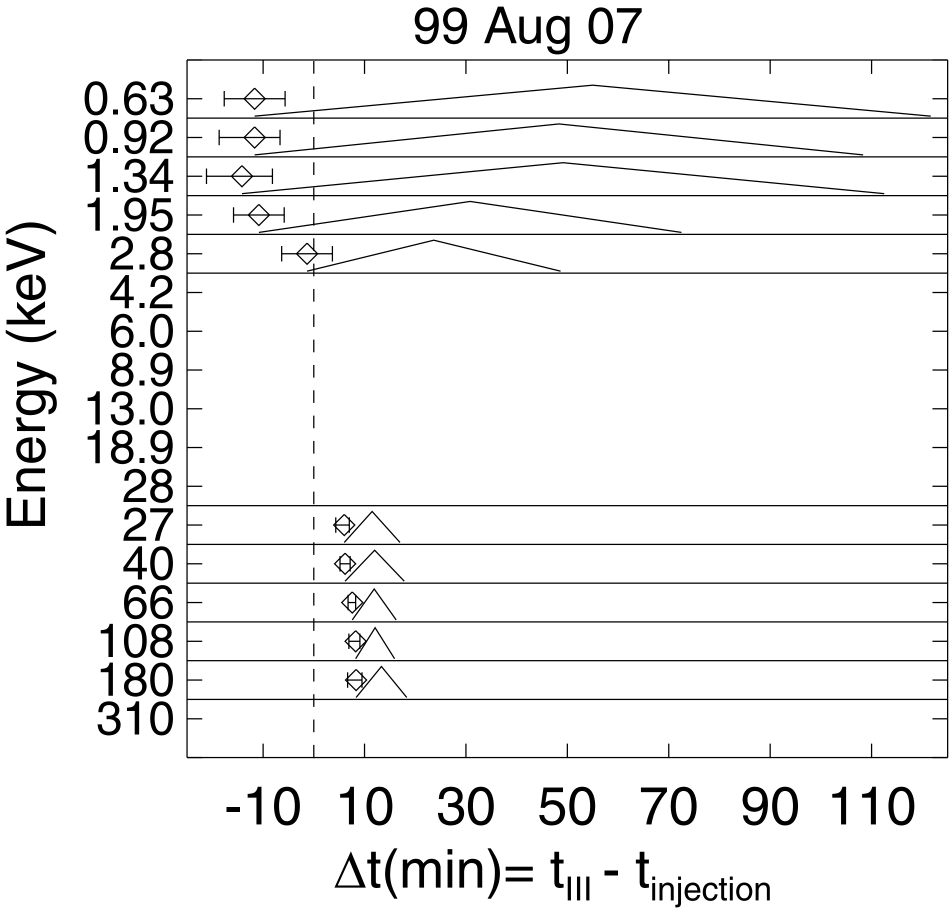

Figure 12. The inferred injection time profiles at the Sun (triangles) from fitting to the time profiles observed by the Wind 3-D P instrument near 1 AU (see Figure 11). The uncertainties in the onset are shown as diamonds with error bars.

The peaks of the injection for ~0.6 to 3 keV electrons, however, are delayed relative to the injection peaks for $\gtrsim$20 keV electrons, and the durations are much longer, ~30–70 minutes. In the same study, the other two scatter-free events with delays at energies $\gtrsim$20 keV also show the same injection characteristics.

Thus, the injection at the Sun of electrons at energies below ~10 keV appears to be the source of the solar type III radio burst, while the delayed injection of $\gtrsim$20 keV electrons points to a second injection, possibly related to a coronal or CME shock wave as suggested by Krucker *et al.* (1999) and Haggerty and Roelof (2002).

It should be noted that many hard X-ray bursts do not have associated type III radio bursts – presumably the electrons are trapped and unable to escape. On the other hand, many type III bursts are not accompanied by hard X-rays – either the electrons are accelerated high in the corona where the ambient density is too low or the number of accelerated electrons is too low for detectable hard X-ray emission. Further more detailed comparisons between RHESSI HXR/γ-ray emission and SEPs observed by ACE, Wind, and other spacecraft will help resolve the relationship between particles at the Sun and in the IPM.

Acknowledgements

I'm pleased to acknowledge useful discussions with D. Smith, S. Krucker, L. Wang at Berkeley; R. Mewaldt at Caltech; and G. Share and R. Murphy at NRL. This research was supported in part by NASA contract NAS5-98033 and grant NAG FDNAG5-11804.

References

Emslie, A. G., Kontar, E. P., Krucker, S., and Lin, R. P.: 2003, *Astrophys. J.* **595**, L107.
Gallagher, P., Dennis, B., Krucker, S., Schwartz, R., and Tolbert, K.: 2002, *Solar Phys.* **210**, 341.
Gopalswamy, N., Xie, H., Yashiro, S., and Usoskin, I.: 2005, *American Geophys. Union Meeting, San Francisco, CA*, Abstract SH23A-0318.
Gosling, J. T., Skoug, R. M., and McComas, D. J.: 2003, *Geophys. Res. Lett.* **30**(13), 1697: 30-1 to 4.
Haggerty, D. K., and Roelof, E. C.: 2002, *Astrophys. J.* **579**, 841.
Hurford, G., Schmahl, E. J., Schwartz, R. A., Conway, A. J., Aschwanden, M. J., Csillaghy, A., *et al.*: 2002, *Solar Phys.* **210**, 61.
Hurford, G., Schwartz, R. A., Krucker, S., Lin, R. P., Smith, D. M., and Vilmer, N.: 2003, *Astrophys. J.* **595**(2), L81.
Hurford, G., Krucker, S., Lin, R. P., Schwartz, R. A., Share, G. H., and Smith, D. M.: 2006, *Astrophys. J.* **644**(1), L93.
Kahler, S.: 2005, *American Geophys. Union Fall Meeting*, San Francisco, CA, Abstract SH21A-07.
Krucker, S., Larson, D. E., Johnson, B. P., and Lin, R. P.: 1999, *Astrophys. J.* **519**, 864.
Krucker, S. and Lin, R. P.: 2002, *Solar Phys.* **210**, 229.
Krucker, S., Hurford, G. J., and Lin, R. P.: 2003, *Astrophys. J.* **595**, L103.
Krucker, S., Lin, R. P., and Kontar, E. P.: 2004, *2004 Joint Assembly*, 17–21 May, Montreal, Canada, paper SH22A-02.
Li, G., Zank, G. P., and Rice, W. K. M.: 2003, *J. Geophys. Res.* **108**(A2), 1082: SSH 10-1 to 10-22.
Lin, R. P.: 1974, *Solar Phys.* **16**, 189.
Lin, R. P. and Hudson, H. S.: 1976, *Solar Phys.* **50**, 153.
Lin, R. P.: 1985, *Solar Phys.* **100**, 537.
Lin, R. P., Anderson, K. A., Ashford, S., Carlson, C., Curtis, D., Ergun, R., *et al.*: 1995, *Space Sci. Rev.* **71**, 125.
Lin, R. P., Larson, D., McFadden, J., Carlson, C. W., Ergun, R. E., Anderson, K. A., *et al.*: 1996, *Geophys. Res. Lett.* **23**, 1211.
Lin, R. P., Feffer, P. T., and Schwartz, R. A.: 2001, *Astrophys. J. Lett.* **557**, L125.
Lin, R. P., and 65 co-authors: 2002, *Solar. Phys.* **210**, 3.
Lin, R. P., Krucker, S., Hurford, G. J., Smith, D. M., Hudson, H. S., Holman, G. D., *et al.*: 2003, *Astrophys. J. Lett.* **595**, L69.

Mewaldt, R. A., Looper, M. D., Cohen, C. M., Mason, G. M., Desai, M. I., Haggerty, D. K., *et al.*: 2005, *2005 Joint Asssembly*, New Orleans, LA, Abstract SH32A-05.

Ramaty, R. and Murphy, R. J.: 1987, *Space Sci. Rev.* **45**, 213.

Shibata, K., Masuda, S., Shimojo, M., Hara, H., Yokoyama, T., Tsuneta, S., *et al.*: 1995, *Astrophys. J. Lett.* **451**, L83.

Smith, D. M., Share, G. H., Murphy, R. J., Schwartz, R. A., Shih, A. Y., and Lin, R. P.: 2003, *Astrophys. J. Lett.* **595**, L81.

Sturrock, P. A.: 1966, *Nature* **211**, 697.

Sui, L. and Holman, G. D.: 2003, *Astrophys. J.* **596**(2), L251.

Wang, L., Lin, R. P., Krucker, S., and Gosling, J. T.: 2006, *Geophys. Res. Lett.* **33**, L03106, doi: 10.1029/2005GL024434.